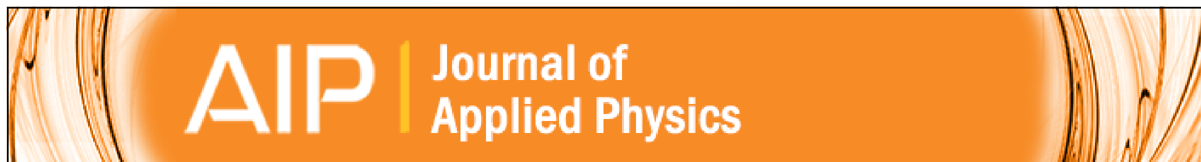


# Xray reflectivity of an Sb deltadoping layer in silicon



W. F. J. Slijkerman, J. M. Gay, P. M. Zagwijn, J. F. van der Veen, J. E. Macdonald, A. A. Williams, D. J. Gravesteijn, and G. F. A. van de Walle



Citation: Journal of Applied Physics 68, 5105 (1990); doi: 10.1063/1.347047
View online: http://dx.doi.org/10.1063/1.347047
View Table of Contents: http://scitation.aip.org/content/aip/journal/jap/68/10?ver=pdfcov
Published by the AIP Publishing

Re-register for Table of Content Alerts

Create a profile.

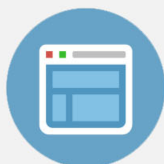

Sign up today!

[This article is copyrighted as indicated in the article. Reuse of AIP content is subject to the terms at: http://scitation.aip.org/termsconditions. Downloaded to ] IP: 131.251.254.28 On: Fri, 21 Feb 2014 10:21:49

# X-ray reflectivity of an Sb delta-doping layer in silicon

W. F. J. Slijkerman, J. M. Gay,[a] P. M. Zagwijn, and J. F. van der Veen
*FOM-Institute for Atomic and Molecular Physics, Kruislaan 407, 1098 SJ Amsterdam, The Netherlands*

J. E. Macdonald and A. A. Williams
*University of Wales, College of Cardiff, Cardiff CF1 3TH, United Kingdom*

D. J. Gravesteijn and G. F. A. van de Walle
*Philips Research Laboratories, P.O. Box 80000, 5600 JA Eindhoven, The Netherlands*

(Received 9 April 1990; accepted for publication 29 June 1990)

X-ray reflectivity measurements were made on Si(001) crystals containing a delta-doping layer of Sb atoms a few nanometers below the surface. The measurements show the Sb doping profile to be abrupt towards the substrate side of the sample and to decay towards the surface with a characteristic decay length of 1.01 nm.

## I. INTRODUCTION

For the structural characterization of sharp, delta-function-shaped,[1] dopant profiles the techniques most frequently used are secondary-ion mass spectroscopy (SIMS) and Rutherford backscattering spectrometry (RBS). SIMS provides a large dynamic detection range of several orders of magnitude in dopant concentration whereas RBS and medium-energy ion scattering (MEIS)[2] can only detect dopant concentrations down to $10^{-2}$ at. % under favorable conditions.[3] However, owing to practical limitations on primary beam energy ($>1$ keV) and angle of incidence ($>80°$) and analyzed area diameter ($>5\,\mu m$) full width at half maxima in SIMS are restricted to at best $\sim 3$ nm (Ref. 4) while resolutions of typically few tenths of a nm[2,5,6] are achieved in MEIS experiments where electrostatic analysis of the backscattered ions is performed.[7]

In this paper we present x-ray reflectivity measurements of an Sb delta-doping layer in Si, revealing the Sb doping profile. In contrast to SIMS and RBS, x-ray reflectivity is a nondestructive technique. It probes the derivative of the electron density as a function of depth of the material under study.[8] This technique is therefore only applicable for high local dopant concentrations. When applicable, x-ray reflectivity provides unprecedented depth resolution but it has a limited dynamic range of typically one decade in concentration. In the case studied here a "spike" of Sb dopant atoms is present in a very high concentration (locally $10^{21}$ Sb atoms/$cm^3$) at a depth of a few nm below the surface.

## II. EXPERIMENT

The reflectivities have been measured for three different samples. Sample B was grown by a method described previously.[9,10] Sb was first deposited on a MBE-grown Si(001) crystal kept at 890 K, followed by deposition of a few nm *a*-Si at room temperature. The *a*-Si overlayer was subsequently crystallized to *c*-Si by heating to 800 K for 3 min. This procedure leads to very narrow doping profiles[9] with the Sb dopant atoms located on substitutional lattice sites. Samples A and C were prepared in exactly the same way, but for sample C only the Sb deposition stage was left out and for sample A the crystallization step at 800 K was not performed. MEIS, performed *in situ* on the samples A and B before the samples were taken out of the vacuum for the x-ray experiments, showed that the total amount of Sb was 0.7 monolayer [one monolayer is defined as the number of atoms in a single Si(001) plane and equals $6.78\times10^{14}$ atoms/$cm^2$]. MEIS done after the x-ray measurements showed that on all samples a thin $SiO_2$ oxide had formed, each of different thickness.

Reflectivity curves for samples B and C were measured in air using the five-circle diffractometer of the wiggler beamline at the Synchrotron Radiation Source in Daresbury (U.K.). The x-rays were monochromatized at a wavelength $\lambda = 0.138$ nm by a channel-cut Si crystal. A highly collimated x-ray beam having a width of 1.0 mm and a height of 3.0 mm was scattered in the horizontal plane from the vertically mounted sample. For specular reflection the wave-vector transfer $Q$ is given by $Q = 2k\sin\theta$, where $\theta$ is the angle of incidence and exit and $k = 2\pi/\lambda$ (Fig. 1). The scattered radiation was collected by a detector positioned at a distance of $D = 750$ mm from the sample, with slits in front defining a horizontal width $w = 0.25$ mm and height $h = 3.0$ mm. This results in an acceptance in $Q$ space of $0.05Q_c$, where $Q_c$, the

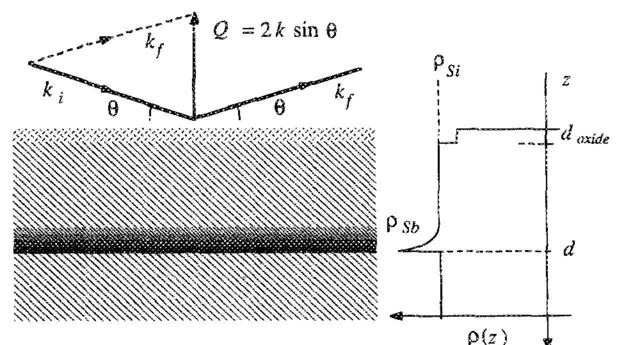


FIG. 1. Specular x-ray reflection from a delta-doping layer of Sb located at a certain depth $d$ in Si. The variation of the density with depth is schematically indicated by the function $\rho(z)$ in the right-hand part.

[a] Permanent address: CRMC2-CNRS, Département de Physique, Faculté des Sciences de Luminy, Case 901, 13288 Marseille Cedex 9, France.

 0021-8979/90/225105-04$03.00 © 1990 American Institute of Physics 

[This article is copyrighted as indicated in the article. Reuse of AIP content is subject to the terms at: http://scitation.aip.org/termsconditions. Downloaded to ] IP: 131.251.254.28 On: Fri, 21 Feb 2014 10:21:49

critical momentum transfer for total reflection, equals 0.315 $nm^{-1}$. The surface area over which the scattering is measured coherently is then given by $\sim D^2\lambda^2/(wh\theta)$,[11] which for the largest $\theta$ value measured is equal to $\sim 3.0\times 10^5$ $nm^2$. The specular reflectivity $R(Q)$ at a given fixed $Q$ was measured by integrating the scattered intensity in a transverse momentum scan in which the crystal is rocked around the axis perpendicular to the scattering plane.

The x-ray reflectivity measurements on sample A were performed using an 18-kW Enraf-Nonius GX-21 x-ray generator. The rotating anode was operated at 40 kV and 140 mA. Cu$K\alpha_1$ radiation of $\lambda = 0.1542$ nm wavelength was reflected from a flat Ge(111) monochromator crystal and selected through slits in front of the sample. A detector, which had slits in front with $w = 0.85$ mm and $h = 10$ mm, was located at a distance of $D = 500$ mm from the vertically mounted sample. For this configuration the $Q$ acceptance is better than $0.05Q_c$. A $\theta$-$2\theta$ scan was made to obtain the reflectivity curve.

## III. RESULTS AND DISCUSSION

The reflectivity curves normalized to the Fresnel reflectivity $R_F(Q)$ are shown in Fig. 2 together with their statistical error of measurement. Curve (c) in Fig. 2 for sample C without Sb shows a monotonic decrease without any features while the doped samples A and B show oscillations extending to the largest $Q$ values measured [curves (a) and (b) in Fig. 2]. Obviously, the oscillations are caused by the presence of the Sb delta-doping layer.

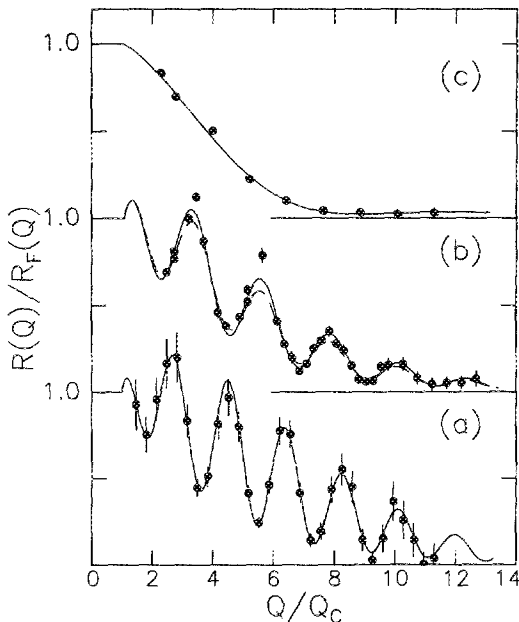


FIG. 2. Measured normalized reflectivities $R(Q)/R_F(Q)$ as a function of $Q/Q_c$. (a) The reflectivity curve obtained for sample A with Sb underneath $a$-Si. The solid curve is the best fit to the data for an exponential profile as shown in Fig. 1. (b) The reflectivity curve for sample B with a Sb delta-doping layer in c-Si. The solid line is the best fit for an exponential Sb profile with a decay length $\sigma_{Sb} = 1.01$ nm. The dashed line is the fit for $\sigma_{Sb} = 1.38$ nm. (c) The reflectivity for sample C without Sb. The solid line is the best fit for a model with only oxide on top of the sample surface.

From the measured reflectivity curves the width of the Sb profile and rms roughness of the overgrown Si layer will be derived. The basic equation for calculation of the reflectivity curve is in the kinematic approximation given by[8]

$$\frac{R(Q)}{R_F(Q)} = \left(\frac{\theta}{A}\right)\left(\frac{Q^2}{4\pi^2}\right) \times \left|\frac{1}{\langle\rho(\infty)\rangle}\int d^3\mathbf{r}\rho(\mathbf{r})e^{-iQ'\cdot\mathbf{r}}\right|^2, \quad (1)$$

where $A$ is the cross-sectional area of the beam, $\langle\rho(\infty)\rangle$ is the average electron density in the bulk, $\rho(\mathbf{r})$ is the electron density at position $\mathbf{r}$, and $Q'$ is the internal wave-vector transfer after refraction at the boundary of the medium. $Q'$ is related to the external wave-vector transfer $Q$ through $Q'^2 = Q^2 - Q_c^2$. If we adopt a coordinate frame in which the $x$ and $y$ directions are in the surface plane and the positive $z$ direction points into the crystal, then for specular reflection the integration over $x$ and $y$ yields, in the case of a short-range gaussian height-height correlation function, a factor[8,12]

$$4\pi^2\left(\frac{A}{\theta}\right)e^{-Q'^2\sigma_s^2}. \quad (2)$$

In this factor, the parameter $\sigma_s$ is the rms surface roughness. The integration over $z$ results in a factor equal to[8]

$$\left(\frac{1}{Q^2}\right)\left|\int\frac{\partial\langle\rho(z)\rangle}{\partial z}e^{-iQ'z}dz\right|^2. \quad (3)$$

Combining (1), (2) and (3) we obtain

$$\frac{R(Q)}{R_F(Q)} = e^{-Q'^2\sigma_s^2}\left|\frac{1}{\langle\rho(\infty)\rangle}\int\frac{\partial\langle\rho(z)\rangle}{\partial z}e^{-iQ'z}dz\right|^2. \quad (4)$$

As an example we calculate $R(Q)/R_F(Q)$ for an exponentially shaped Sb profile. In that case $\rho(z)$ consists of a step function $\theta(z)$ from the substrate which is equal to unity in the crystal and zero elsewhere, plus, at a certain depth $d$, an exponentially shaped Sb profile:

$$\rho(z) = \theta(z) + (P/\sigma_{Sb})e^{(z-d)/\sigma_{Sb}} \quad \text{for } z \leqslant d, \qquad = 1 \quad \text{for } z > d, \quad (5)$$

where $\sigma_{Sb}$ is the $1/e$ decay length of the Sb doping profile and $P$ is a constant given by

$$P = \left(\frac{Z_{Sb} - Z_{Si}}{Z_{Si}}\right)N_{Sb}a_z. \quad (6)$$

$Z_{Sb} = 51$ and $Z_{Si} = 14$ are the atomic numbers of Sb and Si, $N_{Sb}$ is the total amount of Sb in monolayer units, and $a_z$ is the spacing between two atomic (001) planes [for Si(001), $a_z = 0.13577$ nm]. For such a profile Eq. (4) yields

$$\frac{R(Q)}{R_F(Q)} = e^{-Q'^2\sigma_s^2}\left(1 + \frac{Q'^2P^2}{1+Q'^2\sigma_{Sb}^2} - \frac{2PQ'}{1+Q'^2\sigma_{Sb}^2} \times (Q'\sigma_{Sb}\cos Q'd - \sin Q'd)\right). \quad (7)$$

The model predicts an oscillation with period $2\pi/d$. The narrower the profile the larger the amplitude of the oscillations. This statement holds, independent of the exact shape of $\rho_{Sb}(z)$. The prefactors of the cosine and sine terms determine the phase of the oscillation. This phase depends on the



[This article is copyrighted as indicated in the article. Reuse of AIP content is subject to the terms at: http://scitation.aip.org/termsconditions. Downloaded to ] IP: 131.251.254.28 On: Fri, 21 Feb 2014 10:21:49

TABLE I. Optimum parameter values used to fit the experimental reflectivity curves in Fig. 2. In the fit for sample C without Sb only a thin oxide film on top of the sample surface is considered. The surface roughness $\sigma_s$ is obtained from this fit. In the fits for sample B four different models for the Sb profile are considered as indicated. $d_{oxide}$ is oxide thickness, $d$ is the thickness of the Si overlayer, $\sigma_{Sb}$ is the standard deviation of $\rho_{Sb}(z)$ (see Ref. 15). $\chi^2$ is the reduced chi-squared value corresponding to the fits. The symbol * indicates a fixed parameter value.

| | $\sigma_s$ (nm) | $SiO_2$ coverage ($10^{15}/cm^2$) | $d_{oxide}$ (nm) | $d$ (nm) | $\sigma_{Sb}$ (nm) | $\chi^2$ |
|---|---|---|---|---|---|---|
| Sample A (Sb + $a$-Si) | | | | | | |
| exponential | 0.41* | $2.9 \pm 3.2$ | $1.3 \pm 2.5$ | $9.4 \pm 1.2$ | $0.57 \pm 0.37$ | 0.23 |
| Sample B (Sb + $c$-Si) | | | | | | |
| Exponential | 0.41 | 2.2* | $1.07 \pm 0.05$ | $7.35 \pm 0.13$ | $1.01 \pm 0.37$ | 2.03 |
| Half-gaussian | 0.41* | 2.2* | $1.06 \pm 0.05$ | $7.50 \pm 0.13$ | $0.70 \pm 0.15$ | 2.39 |
| Full gaussian | 0.41* | 2.2* | $1.05 \pm 0.05$ | $6.78 \pm 0.12$ | $0.59 \pm 0.13$ | 4.17 |
| Block | 0.41* | 2.2* | $1.05 \pm 0.05$ | $6.78 \pm 0.11$ | $0.52 \pm 0.08$ | 4.39 |
| Sample C (no Sb) | | | | | | |
| | $0.41 \pm 0.12$ | 1.7* | $1.15 \pm 0.08$ | ... | ... | 2.26 |

exact functional form of $\rho_{Sb}(z)$. The overall decrease in intensity is determined by the surface roughness factor in front.

Equation (4) will be used to fit the data but it is not *a priori* obvious that the Sb profile should be exponential. During crystallization of the $a$-Si overlayer (sample B) the Sb profile will broaden due to the interplay of several processes. First, at the crystallization temperature of 800 K the diffusion constant for Sb in $a$-Si is large enough for diffusion to take place.[13] Diffusion of Sb into $c$-Si is ruled out since the corresponding diffusion constant is far too low at 800 K.[14] Second, a moving phase boundary is present. The location of the progressing $a$-Si/$c$-Si interface is given by the product of crystallization velocity and time. On the $a$-Si side of this moving interface, Sb diffusion is possible while on the $c$-Si side it is not. Third, at the moving interface segregation may occur, a process which is characterized by the interfacial segregation coefficient and which is similar to the segregation observed at a $c$-Si/$l$-Si interface during zone refining. The dependence of the Sb profiles on diffusion coefficient, crystallization velocity, and interfacial segregation coefficient will be discussed elsewhere. Here the data are fitted to four different profiles given by analytically Fourier transformable functions. Two of them are functions that are abrupt towards the substrate side and have a tail towards the surface, i.e., an exponential and a half-gaussian function. The other two profiles are symmetric functions, i.e., a gaussian and a block function.

In order to obtain good fits, we have to add an extra contribution to the density profile arising from the $SiO_2$ oxide which formed on top of the sample upon exposure to air (Fig. 1). In the fitting procedures the electron density integrated over the oxide thickness is kept fixed at the value as determined by MEIS. The oxide thickness is left as a free parameter.

For the undoped sample C, constant $P$ is set to zero and the experimental curve is fitted with only three free parameters, namely, the surface roughness $\sigma_s$, the oxide thickness, and an overall scaling factor. The result is shown by the full line through the data points in Fig. 2(c). From the fit $\sigma_s$ is determined to be 0.41 nm. In fitting the experimental reflectivity curves for the samples with the Sb doping layer $\sigma_s$ is fixed at this value. Constant $P$ is fixed at 0.26, which is the value derived from the Sb coverage $N_{Sb}$ of 0.71 monolayer as measured by MEIS. Free parameters are the oxide thickness, the thickness $d$ of the $c$-Si overlayer, the standard deviation $\sigma_{Sb}$ of $\rho_{Sb}(z)$,[15] and an overall scaling factor.

The full line in Fig. 2(b) shows the fit of an exponential profile to the reflectivity curve for sample B. The best-fit parameters for all fits are given in Table I, along with their reduced chi-squared values.[15] The error margins listed in Table I correspond to a change of a given parameter yielding a reduced $\chi^2$ value increased by one with respect to the best-fit $\chi^2$ value with the other parameters relaxed.[15]

From the $\chi^2$ values in Table I it can be seen that both symmetric functions for $\rho_{Sb}(z)$ yield much poorer fits than the exponential and half-gaussian functions. Hence the Sb profile is abrupt towards the substrate side, as is expected. An exponential profile is marginally better than a half-gaussian one. Other choices of profiles yield no improvement in reduced $\chi^2$. We conclude that, within the accuracy of the data, the Sb profile is properly described by an exponential curve with $\sigma_{Sb} = 1.01$ nm.

In fitting the reflectivity curve for sample A the lowest $\chi^2$ was obtained for an exponential Sb profile. Fits to the other three functions yielded significantly higher $\chi^2$ values. The full line in Fig. 2(a) represents the best-fit curve for $\sigma_{Sb} = 0.57$ nm. We see that during $a$-Si crystallization the Sb profile is broadened from 0.57 to 1.01 nm. This result is in agreement with a previous high-resolution ion backscattering study.[9]

The depth resolution and sensitivity to the precise form of the dopant profile are limited by the accuracy of the data and by the experimentally accessible range of $Q$ values. The finite $Q$ range probed yields a cutoff in the Fourier representation of the density [Eq. (1)], which results in a finite reso-



[This article is copyrighted as indicated in the article. Reuse of AIP content is subject to the terms at: http://scitation.aip.org/termsconditions. Downloaded to ] IP: 131.251.254.28 On: Fri, 21 Feb 2014 10:21:49

lution in real space.[16] The depth resolution in our experiment we estimate to be 0.37 nm; to illustrate our sensitivity to the parameter $\sigma_{Sb}$, we compare in Fig. 2(b) the best-fit curve for $\sigma_{Sb} = 1.01$ nm with a curve calculated for $\sigma_{Sb} = 1.38$ nm. The $\chi^2$ value for the latter curve is 1.0 larger than for the best-fit curve. The depth resolution can be improved by extending the $Q$ range of the measurements and improving the counting statistics.

We have shown that x-ray reflectivity measurements of delta-doping profiles may even be performed on a rotating anode x-ray generator where count rates are generally much lower than at a synchrotron radiation source. On the rotating anode a count rate of 0.15 counts/s with a background of 0.12 counts/s was obtained for the largest $Q$ value of $Q = 11.3Q_c$. This has to be compared with a count rate of 3.5 counts/s with a background of 2.2 counts/s obtained with unfocused synchrotron radiation for the same $Q = 11.3Q_c$. The larger statistical uncertainties resulting from the lower count rate cause the reduced $\chi^2$ value to be lower and the error margins on the best-fit parameters to be larger for sample A than for sample B.

In conclusion, x-ray reflectivity is a useful nondestructive tool for the characterization of high-concentration delta-doping profiles. We showed the presence of an exponentially shaped profile of Sb in $c$-Si with a $1/e$ decay length of $1.01 \pm 0.37$ nm.

## ACKNOWLEDGMENTS

We would like to thank the staff of Daresbury Laboratory for assistance during the measurements. P. Lambooy is gratefully acknowledged for assistance with operating the rotating anode x-ray generator. This work is part of the research program of the Stichting voor Fundamenteel Onderzoek der Materie (FOM) and was made possible by financial support from the Nederlandse Organisatie voor Wetenschappelijk Onderzoek (NWO) and Philips Research Laboratories (Eindhoven).

[1] M. A. Herman, and H. Sitter, *Molecular Beam Epitaxy* (Springer, Berlin, 1989).
[2] J. F. van der Veen, Surf. Sci. Rep. **5**, 199 (1985).
[3] W. K. Chu, J. W. Mayer, and M. A. Nicolet, *Backscattering Spectrometry* (Academic Press, New York, 1978).
[4] J. B. Clegg, and R. B. Beall, Surf. Interface Anal. **14**, 307 (1989).
[5] E. J. van Loenen, J. F. van der Veen, and F. K. Legoues, Surf. Sci. **157**, 1 (1985).
[6] W. F. J. Slijkerman, A. E. M. J. Fischer, J. F. van der Veen, I. Ohdomari, S. Yoshida, and S. Misawa, J. Appl. Phys. **66**, 666 (1989).
[7] R. G. Smeenk, R. M. Tromp, H. H. Kersten, A. J. H. Boerboom, and F. W. Saris, Nucl. Instrum. Methods **195**, 581 (1982).
[8] A. Braslau, P. S. Pershan, and G. Swislow, B. M. Ocko, and J. Als-Nielsen, Phys. Rev. A **38**, 2457 (1988).
[9] W. F. J. Slijkerman, P. M. Zagwijn, J. F. van der Veen, A. A. van Gorkum, and G. F. A. van de Walle, Appl. Phys. Lett. **55**, 963 (1989).
[10] A. A. van Gorkum, K. Nakagawa, and Y. Shiraki, J. Appl. Phys. **65**, 2485 (1989).
[11] A. Braslau, M. Deutsch, P. S. Pershan, A. H. Weiss, J. Als-Nielsen, and J. Bohr, Phys. Rev. Lett. **54**, 114 (1985).
[12] S. K. Sinha, E. B. Sirota, S. Garoff, and H. B. Stanley, Phys. Rev. B **38**, 2297 (1988).
[13] H. Matsumara, M. Maeda, and S. Furukawa, J. Non-Cryst. Solids **59&60**, 517 (1983); Jpn. J. Appl. Phys. **22**, 771 (1983).
[14] C. T. Lynch, *Handbook of Materials Science* (Chemical Rubber Company, Cleveland, 1975), Vol. 3
[15] P. R. Bevington, in *Data Reduction and Error Analysis for the Physical Sciences* (McGraw-Hill, New York, 1969).
[16] H. Lipson and W. Cochran, *The Determination of Crystal Structures*, 3rd ed. (Cornell University Press, Ithaca, New York, 1966), Chap. 12, pp. 317–357.



[This article is copyrighted as indicated in the article. Reuse of AIP content is subject to the terms at: http://scitation.aip.org/termsconditions. Downloaded to ] IP: 131.251.254.28 On: Fri, 21 Feb 2014 10:21:49